Available online at www.sciencedirect.com
ScienceDirect
Thermochimica Acta 467 (2008) 99–106
thermochimica acta
www.elsevier.com/locate/tca

Nonisothermal kinetic analysis of the effect of protein concentration on BSA aggregation at high concentration by DSC

Xiaomin Cao [a], Jie Li [a], Xi Yang [a], Yun Duan [a], Yuwen Liu [a,b,*], Cunxin Wang [a]

[a] *College of Chemistry and Molecular Science, Wuhan University, Wuhan 430072, Hubei, China*
[b] *College of Life Science, Wuhan University, Wuhan 430072, Hubei, China*

Received 2 August 2007; received in revised form 13 November 2007; accepted 15 November 2007
Available online 22 November 2007

Abstract

The effect of protein concentration on bovine serum albumin (BSA) aggregation kinetics at high concentration was studied by differential scanning calorimetry (DSC). The nonisothermal kinetic analysis of this process was carried out using a composite procedure involving the iso-conversional method and the master plots method. The observed aggregation process was characterized by denaturation temperature ($T_{d\,max}$), apparent activation energy (E), the apparent order of reaction (n), and pre-exponential factor (A) which all increased with the increase of BSA concentration. The results suggested that the apparent aggregation reaction of BSA approximately conformed to the simple order reaction model. The higher BSA concentration, the higher the apparent order of reaction and the more close to 2 was. The difference intrinsic fluorescence of BSA between before and after the thermal denaturation and aggregation provided the evidences of conformation changes of BSA and the substantial impact of BSA concentration on aggregation. This study showed the combination of iso-conversional method and the master plots method could be used to model the aggregation mechanism of the protein.

Keywords: DSC; BSA; Nonisothermal kinetics analysis; The iso-conversional method and the master plots method; Aggregation

1. Introduction

Proteins often exist in their physiological environment at high concentrations or in crowded environments. Hemoglobin, for example, is found in erythrocytes at concentrations exceeding 300 g l^{-1}, and serum albumin is present in blood in the range of 35–55 g l^{-1} [1]. In 1977, Ross and Minton demonstrated that dramatic nonideality arises in the thermodynamic activity of hemoglobin in salt solutions with increasing protein concentrations [2]. Despite the increasing relevance of highly concentrated protein solutions, the unfolding and aggregation of proteins at high concentrations are incompletely understood. In biological systems it is required for the assembly of structures with specific functions such as microtubules, blood clots, and viral coatings. The aggregation of proteins is, in general, triggered by a conformational change of the protein induced by heat, enzymatic cleavage, or other processes that affect the folded structure. After this change of structure, a series of reactions take place that lead to the formation of aggregates [9]. Aggregation of protein is an important process in many biological systems and industrial processes.

Bovine serum albumin (BSA) is a relatively large globular protein (about 66 kDa) with well-characterized physiochemical properties [11,12]. Although extensive literatures have been published on the experimental and theoretical aspects of BSA denaturation with urea, guanidine hydrochloride as denaturing agents, increasing of temperature and changes in pH or ionic strength [3–9] based on the Lumry–Eyring model [10], almost all of them [13–17] dealt with the protein unfolding and aggregation at very low concentration, such as 0.5–1.0 mg ml^{-1}, very little information is available on the kinetic aspect of these processes at high concentration. Sánchez-Ruíz method [13] based on the Lumry–Eyring model which studies the processes at very low concentration may not fit the ones at high concentration. So method that can be used directly to analyze the aggregation mechanism of protein at high concentration is thus necessary.

* Corresponding author at: College of Chemistry and Molecular Science, Wuhan University, Wuhan, 430072, Hubei, China. Tel.: +86 27 87218614; fax: +86 27 68754067.
E-mail address: ipc@whu.edu.cn (Y. Liu).

0040-6031/$ – see front matter © 2007 Elsevier B.V. All rights reserved.
doi:10.1016/j.tca.2007.11.009

Although Despa et al. [18] had examined the effects of crowding on the thermal stability of heterogeneous protein solutions; they mainly started from the thermodynamics to study the protein denaturation in a crowded environment. Kinetic analysis of the aggregation of protein at high concentration is very complex. Generally speaking, correlative parameters can be obtained starting from model and combining experiment results. But it is necessary to emphasize that setting up model must depend on experiment results. The kinetic integral "model-free" method can gain kinetic parameters starting from experiment results. And base on this method, a more detailed model can be analyzed. Theoretically, one such as Baier [20,21] could expect that a single experiment in nonisothermal regime could give all the kinetic triplets [19], namely, kinetic model, activation energy and pre-exponential factor. However, the estimations based on fitting data to single-step kinetic models work poorly, and tend to be misleading, especially when these estimates are obtained from nonisothermal measurements [22]. More and more evidences show that kinetic methods that use single heating rate data are limited in their applicability. As an alterative, one may make use of model-free approaches represented by various isoconversional methods to give excellent results of dependencies of the activation energy on the extent of conversion of nonisothermal experiments. For complex reactions of which the mechanism is unknown, the integral "model-free" method is very useful since no model has to be pre-selected in the evaluations of kinetic parameters. And the master plots method will give more insight into the mechanism. Analysis of the activation energy dependency will provide important clues on reaction mechanism [23–26]. Also, the ability of iso-conversional methods to reveal the reaction complexity is, therefore, a crucial step toward the ability to draw mechanistic conclusions from kinetic data. Just as Vyazovkin et al. [27] said, there were numerous applications in kinetic analysis of thermally stimulated processes in synthetic polymers, however, there appeared to be no literature reports on the application of these methods to the thermal denaturation of proteins. Theoretical master plots are reference curves depending on the kinetic models but generally independent of kinetic parameters of the process. Experimental master plots constructed on the basis of experimental data are independent from the temperature schedules. Comparing experimental master plots with theoretical ones allows us to choose the appropriate kinetic model of the process under investigation, at least, of the type of appropriate kinetic models, without doubt [28]. The knowledge of kinetic model, deduced from such a simple graphical method, is very helpful for further detailed kinetic analysis by avoiding a probable miscalculation of kinetic parameters due to wrong model being assumed.

One objective of this study is to develop kinetic model for BSA aggregation at high concentration using the integral "model-free" method and the present work derives a nonisothermal kinetic [29] analysis to extract meaningful kinetic parameters from a system that is predominantly irreversible. And the other aim is to study the effect of BSA concentration on aggregation kinetics at high concentration.

2. Theoretical approach

The theory refers to the literature reported by Tang et al. [30]. To obtain α (conversion of reaction), the following equations are used: in differential scanning calorimetry (DSC), $\alpha = \Delta H_{\text{part}}/\Delta H_{\text{tot}}$, ΔH_{part} is the partial area (J g^{-1}) and ΔH_{tot} is the total peak area (J g^{-1}).

For a reaction under dynamic condition, the differential Arrhenius equation and its integral form give the rate and degree of conversion.

$$\frac{d\alpha}{dt} = \left(\frac{A}{\beta}\right) \exp\left(\frac{-E}{RT}\right) f(\alpha) \tag{1}$$

$$G(\alpha) = \left(\frac{AE}{\beta R}\right) P(u) \tag{2}$$

where α is the extent of conversion, β is the linear heating rate, $f(\alpha)$ or $G(\alpha)$ is the function of degree of conversion in a differential form or an integral form, and $P(u) = \int_{\infty}^{u} -(e^{-u}/u^2)\,du$, $u = E/RT$. Unfortunately, P (u), also called the "temperature integral", cannot be analytically integrated. To solve this problem, an approximate formula of high accuracy [31] is introduced into Eq. (2), and taking the logarithms of both sides, the following equation is obtained as

$$\ln\left(\frac{\beta}{T^{1.894661}}\right) = \ln\left[\frac{AE}{RG(\alpha)}\right] + 3.635041 - 1.894661 \ln E - 1.001450\frac{E}{RT} \tag{3}$$

For a single-step process with an invariant $G(\alpha)$ expression, an analysis using the master plots delivers an unambiguous choice of the appropriate kinetic model [29,32]. Taking a single-step process into account, the kinetic triplets, i.e. the kinetic model, A and E, are invariable. Using a reference at point $\alpha = 0.5$ and according to Eq. (2), one gets

$$G(0.5) = \left(\frac{AE}{\beta R}\right) P(0.5) \tag{4}$$

where $u_{0.5} = E/RT_{(0.5)}$. The following equation is obtained by dividing Eq. (2) by Eq. (4)

$$\frac{G(\alpha)}{G(0.5)} = \frac{P(u)}{P(u_{0.5})} \tag{5}$$

Plotting $G(\alpha)/G(0.5)$ against corresponds to theoretical master plots of various $G(\alpha)$ functions. In order to draw the experimental master plots of $P(u)/P(u_{0.5})$ against α from experimental data obtained under any heating rates, the knowledge of temperature as a function of α and the value of E for the process should be known in advance. The temperature integral, $P(u)$, has no analytical solution and can be expressed by an approximation, which gives a high accuracy [33].

$$P(u) = \frac{\exp(-u)}{u(1.00198882u + 1.87391198)} \tag{6}$$

The experimental master plot is independent of the heating schedule. Eq. (4) indicates that, for a given α, the experimental value of $P(u)/P(u_{0.5})$ and theoretically calculated values of

$G(\alpha)/G(0.5)$ are equivalent when an appropriate kinetic model is used. This integral master plots method can be used to determine the reaction kinetic models of the reactions.

3. Materials and methods

3.1. Materials

BSA (Fraction V, purity>99.9%, Roche Chemical Company) was used without further purification. Distilled and deionized water was used for the preparation of all solutions. The pH of the buffer (20 mM Na_2HPO_4, 20 mM NaH_2PO_4 and 150 mM NaCl solution) was 6.89 measured by a pH meter (Orion 828). The BSA solutions were prepared by dispersing powdered protein into the buffer.

3.2. Differential scanning calorimetry

The calorimetric experiments were performed in a Mettler Toledo calorimeter, model DSC 822^e, using 160 μl medium pressure crucibles with 120 μl of sample in sample cell (or 100 μl crucibles with 80 μl sample) and the corresponding buffer in reference cell for each particular condition; the instrument was calibrated with indium. Scanning calorimetry measurements were performed with the Star® evaluation program, at different heating rates of 1.0, 1.5, 2, and 2.5 K min^{-1} in the temperature range 35–95 °C. After the end of the first heating round, the protein sample was quickly cooled to 35 °C, and rescanned after 5 min stabilization time at 35 °C. The sample was heated at a low heating rate (<2.5 K min^{-1}) to avoid thermal interference due to circulating convection currents in the sample vessel [34]. Measurements were carried out on three separate samples (replicates) and reported as the average.

3.3. Fluorescence measurements

The fluorescence measurements were performed on an LS-55 PerkinElmer spectrofluorimeter at ambient temperature. The tryptophan fluorescence emission spectra of BSA were measured by exciting at 297 nm. The emission spectra before BSA thermal denaturation and aggregation were studied at five different concentrations of protein, namely 5, 10, 20, 30 and 60 mg ml^{-1}. The sample after the DSC scan was diluted into buffer to 1 ml solution and then measured the tryptophan fluorescence emission spectra at room temperature.

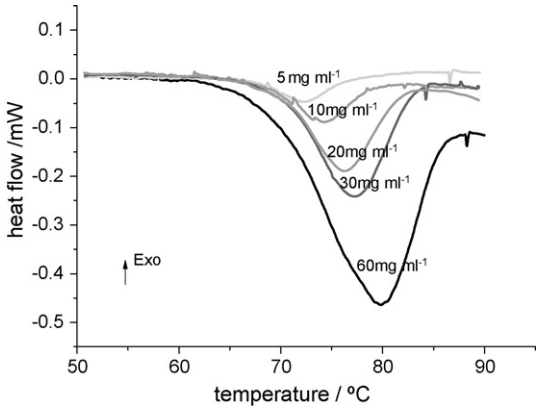

Fig. 1. DSC curves for the influence of protein concentrations on the thermal denaturation and aggregation of BSA (solution pH 6.89) at 2.5 K min^{-1} heating rate after baseline subtraction.

4. Results and discussion

A different measurement was obtained by completing two sequential scans for a single sample. The first scan was completed to denature the protein and only one endothermic peak was found. In this respect, it is noteworthy that the thermal profiles of additional scans (i.e., a third scan) of the denatured samples were essentially identical to that of the second scan, denoting that a single irreversible transition occurred over the temperature range of interest. The repeat curves served as the baseline and were subtracted from the first measurement curves, respectively. Thermograms were evaluated using Star® program. After baseline correction, integral (mJ), and temperature at maximum heat flux $T_{d\,max}$ (K) were recorded for each analysis and the $T_{d\,max}$ at different rates and different BSA concentrations was listed in Table 1. The conversion (α) was calculated using the Star® software [35], and the conversion graph and table (inclusion the corresponding denaturation temperature (T_d)) were also displayed.

The DSC transitions were calorimetrically irreversible and the protein samples extracted from the calorimetric cell showed strong aggregation. BSA denaturation is irreversible probably due to the occurrence of "side" processes such as aggregation [36]. Due to denaturation, hydrophobic interaction can occur, and exposed thiol groups can form disulfide bonds, which result in an irreversible behavior [37,38]. DSC curves of different BSA concentrations at heating rate 2.5 K min^{-1} are displayed in Fig. 1. It distinctly revealed that BSA concentration substantially

Table 1
$T_{d\,max}$ (°C) at different scanning rates

Concentration (mg ml^{-1})	Scanning rate (K min^{-1})			
	1	1.5	2	2.5
10	72.30 ± 0.08[a]	72.96 ± 0.06	73.59 ± 0.05	73.89 ± 0.11
20	73.94 ± 0.02	74.66 ± 0.20	74.93 ± 0.06	75.51 ± 0.06
30	75.08 ± 0.11	75.74 ± 0.15	76.27 ± 0.12	76.92 ± 0.30

Standard deviations $S = \sqrt{\sum (X - M)^2/(n-1)}$, where $\sum$ is the sum of, X is the individual score, M is the mean of all scores and n is the sample size (number of scores).

[a] Means ± standard deviations.

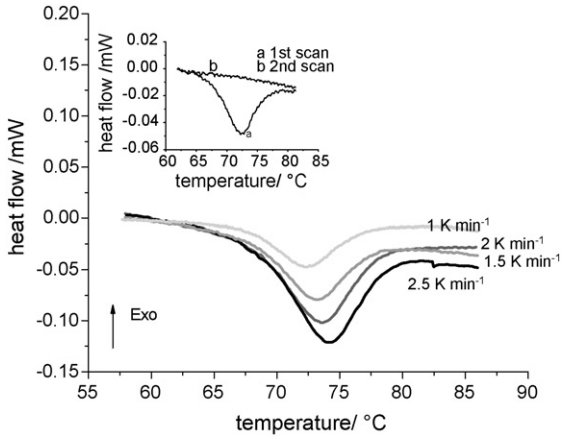

Fig. 2. DSC curves for 10 mg ml^{-1} BSA in 20 mM sodium phosphate with 150 mM NaCl (pH 6.89) at different heating rates. From the top to bottom, the scanning rates are 1, 2, 1.5, and 2.5 K min^{-1}, respectively. Inset: DSC scans for irreversible BSA system. The calorimetric transitions were observed to be irreversible as reflected by the lack of transition in the second run of all the samples and the temperature at maximum heat flux, $T_{d\,max}$ of the protein increased with increasing scan rate.

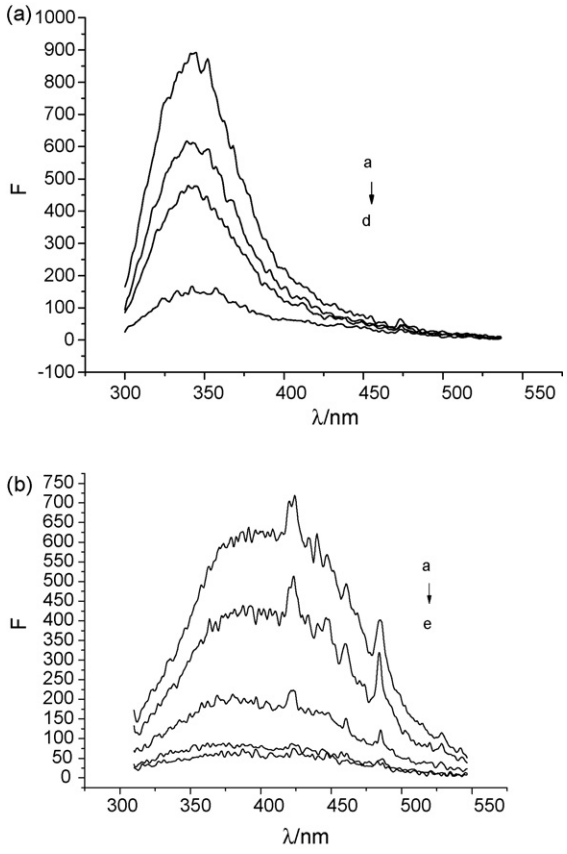

Fig. 3. (A) Emission spectrum of BSA at different protein concentrations: (a) 60 mg ml^{-1}, (b) 30 mg ml^{-1}, (c) 20 mg ml^{-1}, and (d) 5 mg ml^{-1}. Fluorescence excitation wavelength was 297 nm; the excitation slit was set at 10.0 nm and the emission slit was set 5.5 nm. (B) Emission spectrum of BSA after DSC scans: (a) 30 mg ml^{-1}, (b) 20 mg ml^{-1}, (c) 10 mg ml^{-1}, (d) 5 mg ml^{-1}, and (e) 60 mg ml^{-1} dilution. Fluorescence excitation wavelength was 297 nm; the excitation slit was set at 10.0 nm and the emission slit was set 4.0 nm.

affected its thermal denaturation and aggregation—the $T_{d\,max}$ was highly dependent on BSA concentration, which increased from 72.46 to 79.79 °C with the increase of BSA concentration from 5 to 60 mg ml^{-1}. The ΔH (area under the peak) decreased as BSA concentration decreased.

DSC curves of 10 mg ml^{-1} BSA at various heating rates are also shown in Fig. 2. As the heating rate increased, an upward shift occurred in $T_{d\,max}$ of the endothermic peaks was observed and an increase in total enthalpy change was substantial. This would indicate that slower heating rates lead to a gel structure in which bonding are more numerous and a more energetically favorable structure is attained [39]. The $T_{d\,max}$ was highly dependent on the scan rate—an increase in the $T_{d\,max}$ with the increase of scan rate, indicated that the thermal denaturation and aggregation process was, at least in part, under kinetic control. The process may be partially consistent with the proposed model by Lumry and Eyring [10] $N \rightleftharpoons D \rightarrow I$ where N is the native state, D the unfolded one, and I a final state, irreversibly arrived at from D.

The ΔH of 5 mg ml^{-1} BSA thermal denaturation and aggregation at 2.5 K min^{-1} is not high (Fig. 1). And it will be even lower at 1 K min^{-1} and thus bring calculation errors. The evidence for this was the kinetics analysis of the enthalpy changed as a function of heating rate, which occurred during the thermal process. The 60 mg ml^{-1} BSA DSC curve—the peak such as peak temperatures, peak height and peak width at 1 K min^{-1} changed no orderliness (data and cure are not displayed). So concentrations of 10, 20, and 30 mg ml^{-1} were selected for study.

The fluorescence of serum albumin is due to tyrosine and tryptophan residues. The change in the relative fluorescence of serum albumin can be correlated with changes in its structure [40]. A change in the microenvironment surrounding the tryptophan residue can cause the shift of the wavelength of the maximum tryptophan fluorescence emission (λ_{max}) [41]. In most proteins, a red shift of the fluorescence spectra is resulted from the change in the tryptophan microenvironment to a more exposed and a more polar one in the unfolded form [42]. Therefore, the effect of BSA concentration on thermal denaturation and aggregation in the environment of the tryptophan residues can be obtained by measuring the changes in the tryptophan fluorescence spectra.

Fig. 3A gives the fluorescence emission spectra of BSA at varying protein concentrations before DSC scans and Fig. 3B gives the emission spectra of BSA after DSC scans. No shift in λ_{max} was observed in the intrinsic fluorescence of BSA (Fig. 3A) before DSC scans with increase in the concentration of the protein. It supported that there was no change in the extent of aggregation with increase in BSA concentration at ambient temperature. The thermal denaturation and aggregation is accompanied by a red shift of about 75 nm in the emission spectra (Fig. 3A and B). The changes in BSA emission properties after DSC scans are displayed in Fig. 3B. It can be seen that position of the peak changed with the increase of BSA concentration and the shoulder peak boosted up. The λ_{max} values were appreciably red-shifted and the λ values of the shoulder peak were blue-shifted a little at the same time with increase in BSA concentration. But the fluorescence intensity of 60 mg ml^{-1} dilution

Table 2
The apparent activation energy (E) and the correlation coefficients (r) of linear regression at different conversions (α)

α	E (kJ mol^{-1})	r
0.2	532.45	0.99063
0.3	542.58	0.99723
0.4	540.89	0.99926
0.5	535.37	0.99985
0.6	532.76	0.99998
0.7	531.44	0.99972
0.8	534.96	0.99859

almost decreased to zero suddenly. The changes in the tryptophan fluorescence suggested that protein concentration could affect the tryptophan environment during BSA thermal denaturation and aggregation.

4.1. Nonisothermal kinetics for the BSA aggregation at 10 mg ml^{-1}

4.1.1. Iso-conversional method for estimating the activation energy dependence

It is well known that the iso-conversional method can easily give estimate of activation energy regardless of reaction mechanism [22,43]. Using the α–T data obtained from DSC conversion plots, according to Eq. (3), the apparent activation energy of BSA aggregation listed in Table 2 was estimated from the iso-conversional plot of $\ln(\beta/T^{1.894661})$ versus $1/T$ at different conversion ratios (α) in the range of 0.2–0.8. As displayed in Table 2, all these plots have linear correlation coefficients larger than 0.99.

As shown in Fig. 4, the value of activation energy hardly varies with the degree of conversion and the average value of activation energy is 535.38 ± 4.53 kJ mol^{-1}. This is comparable to the activation energy found for other proteins, such as ovalbumin [44], *Rapana thomasiana* (marine snail, Gastropod) hemocyanin [45], β-lactoglobulin [46], wild type nitrite reductase [47], bovine fibrinogen [48], muscle creatine kinase [49], glucose transporter GLUT1 [50]. The large value of E might be expected, because the highly cooperative nature of the protein implies a large ΔH between the folded and denatured protein, and E is always larger than ΔH [44,51]. Due to the little dependence of the activation energy on the extent of conversion, a simple reaction mechanism could be used for reaction progressing.

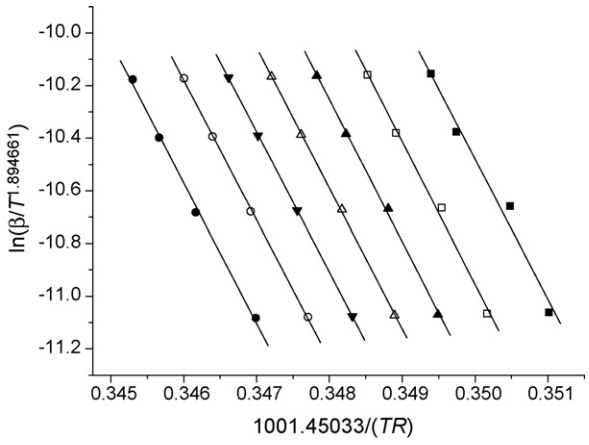

Fig. 4. Plots for determination of activation energy of BSA aggregation at different α: 0.2 (■), 0.3 (□), 0.4 (▲), 0.5 (△), 0.6 (▼), 0.7 (◯), and 0.8 (●). Solid lines are linear fitting corresponding to different α.

However, as mentioned earlier, recently Vyazovkin et al. [27] have researched the thermal denaturation of collagen by iso-conversional method and observed a strong decrease of E with conversion that was consistent with the Lumry–Eyring model. And it discussed in detail a relationship between the Lumry–Eyring model and iso-conversional dependence of E.

The distinctness of study reaction systems and experiment conditions maybe led to different results. In Vyazovkin research, the study system was wet collagen and the value of K fell outside the limiting cases. While in our case, the study systems were high concentration BSA solutions; DSC transitions were strongly scanning rate-dependent; the scanning rate and protein concentration effected on the $T_{\mathrm{d\,max}}$ values; all the thermal transitions were found calorimetrically irreversible and the protein samples extracted from the calorimetric cell showed strong aggregation; the rate limiting step might always be the irreversible process itself as α in the range of 0.2–0.8 (for a strongly rate-limited, irreversible DSC transition, protein concentration effects may occur if the kinetics of the irreversible process is not first order [52,53]), in other words, the value of K always fell inside the limiting case. So, in this case a constant E could be observed. But it must be to point out that aggregation was probably one of the main causes of irreversibility in the thermal transitions of BSA. Therefore, the inactivation kinetics might be expected to have a higher than one reaction order [54].

4.1.2. Master-plots method for determining kinetic model

To determine the most possible mechanism, 18 basic model functions in Table 3 were tested. According to the value of E, the

Table 3
The 18 model functions for the determination of the most probably model function

No.	Reaction model	Symbol	$G(\alpha)$
1	Avrami–Erofeyev ($m = 4$)	A_4	$[-\ln(1-\alpha)]^{1/4}$
2	Avrami–Erofeyev ($m = 3$)	A_3	$[-\ln(1-\alpha)]^{1/3}$
3	Avrami–Erofeyev ($m = 2$)	A_2	$[-\ln(1-\alpha)]^{1/2}$
4	Avrami–Erofeyev ($m = 1.5$)	$A_{1.5}$	$[-\ln(1-\alpha)]^{2/3}$
5	Phase boundary reaction ($n = 1$)	R_1	α
6	Phase boundary reaction ($n = 2$)	R_2	$1-(1-\alpha)^{1/2}$
7	Phase boundary reaction, $n = 3$	R_3	$1-(1-\alpha)^{1/3}$
8	One-dimensional diffusion	D_1	$(1/2)\alpha^2$
9	Two-dimensional diffusion	D_2	$(1/2)[1-(1-\alpha)^{1/2}]^{1/2}$
10	Three-dimensional diffusion	D_4	$1-2\alpha/3-(1-\alpha)^{2/3}$
11	Jander's type diffusion	D_3	$[1-(1-\alpha)^{1/3}]^2$
12	Power law ($n = 1/4$)		$\alpha^{1/4}$
13	Power law ($n = 1/3$)		$\alpha^{1/3}$
14	Power law ($n = 1/2$)		$\alpha^{1/2}$
15	Power law ($n = 3/2$)		$\alpha^{3/2}$
16	First order	A_1, F_1	$-\ln(1-\alpha)$
17	Second order	F_2	$(1-\alpha)^{-1}-1$
18	Third order	F_3	$(1/2)[(1-\alpha)^{-2}-1]$

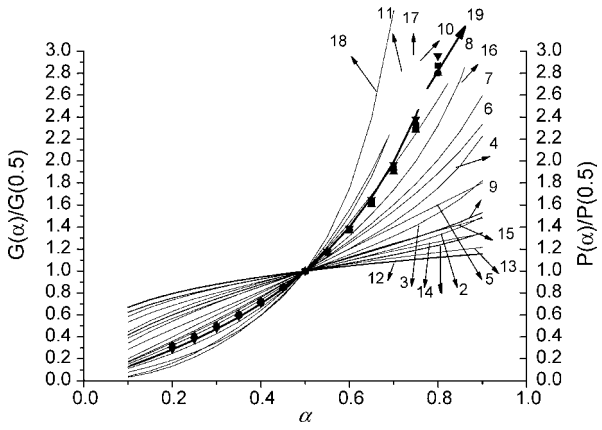

Fig. 5. Master plots of theoretical $P(u)/P(u_{0.5})$ against α for various reaction models (solid curves, as enumerated in Ref. [28], and curve 19 represents function $G(\alpha) = 1/(1-1.5) - (1-\alpha)^{1-1.5}/(1-1.5)$) and experimental data for the 10 mg ml^{-1} BSA aggregation at heating rates 1 K min^{-1} (▲), 1.5 K min^{-1} (▼), 2 K min^{-1} (■), and 2.5 K min^{-1} (●). Models that have been used to describe the simple order reaction process are labeled as: (16) first-order reaction model; (17) second-order reaction model; (18) third-order reaction model.

theoretical master plots of $G(\alpha)/G(0.5)$ versus α and the experimental master plots of $P(u)/P(u_{0.5})$ versus α are obtained, as shown in Fig. 5. The superposition of experiment master plotted at different heating rates indicated that the kinetics process of aggregation of the BSA could be described by a single model function. It can be easily seen from Fig. 5 that the kinetic process for the BSA aggregation is most probably described by F_n model,

$$G(\alpha) = \frac{1}{1-n} - \frac{(1-\alpha)^{1-n}}{1-n}$$

Model F_n represents the chemical kinetics with reaction order n, which reflects the influence degree of concentration on the reaction. The higher of n, the deeper of concentration influence is. Because the experimental master plots lay between the theoretical master plots F_1 and F_2, it was likely that the apparent mechanism of overall reaction could not be expressed in terms of an integral order reaction model, which maybe indicated mixture basic reactions participated in the system.

4.1.3. Evaluation of pre-exponential factor and kinetic exponent

The accommodated F_n model with a nonintegral exponent, which could describe the observed aggregation process, was suggested by the comparison of the experimental master plots with theoretical ones. Also, the kinetic exponent and pre-exponential factors were determined by further calculations. The expression of F_n was introduced into Eq. (2), the following equation was obtained.

$$\frac{1}{1-n} - \frac{(1-\alpha)^{1-n}}{1-n} = \frac{AE}{\beta R} P(u) \tag{7}$$

In Eq. (7), $P(u)$ could be calculated according to Eq. (6). Plotting $(1/(1-n)) - ((1-\alpha)^{1-n}/(1-n))$ versus $E/\beta RP(u)$ from $n = 1$ to 2 with a step of 0.1, a series of straight lines through zero were obtained. The most reasonable exponent n was the one with the highest linear correlation coefficient. Our calculation showed that $n = 1.5$ led to the highest linear correlation coefficient 0.99966 with $A = 4.74\text{E}80\ \text{s}^{-1}$ from the slope of the line. All the apparent kinetic parameters that determined during the main stage of BSA aggregation are summarized in Table 4, and the reported E value corresponded to the average of E values, which were calculated in the α range 0.2–0.8. As shown in Table 4, the class of kinetic models, F_n, can describe the observed aggregation process of BSA.

4.2. Kinetic triplets for BSA aggregation at other concentrations

The same procedures were repeated for the aggregation of BSA solutions at other concentrations 20 and 30 mg ml^{-1}. The activation energies were nearly independent of conversion and the mean activation energy was 537.85 ± 20.66 and 547.14 ± 6.94 kJ mol^{-1}, respectively. Further calculations indicated that the class of kinetic models, F_n, best described the aggregation of BSA solutions at 20 and 30 mg ml^{-1}. Their logarithmic values of pre-exponential factors and kinetic exponents are also presented in Table 4.

It can be concluded from Table 4 that the possible mechanism for the aggregation of BSA solutions at high concentration was simple order reaction. The measurements suggested that the possible forms of $G(\alpha)$ for the aggregation of BSA solutions at high concentration were

for 10 mg ml^{-1},

$$\frac{1}{1-1.5} - \frac{(1-\alpha)^{1-1.5}}{1-1.5}$$

Table 4
Kinetic model and parameters for the apparent BSA aggregation at different concentrations

Concentration (mg ml^{-1})	E (kJ mol^{-1})	A (s^{-1})	n	r	$G(\alpha)$
10	535.38 ± 4.53[a]	4.74E80	1.5	0.99966	$\frac{1}{1-1.5} - \frac{(1-\alpha)^{1-1.5}}{1-1.5}$
20	537.85 ± 20.66	6.07E80	1.7	0.99618	$\frac{1}{1-1.7} - \frac{(1-\alpha)^{1-1.7}}{1-1.7}$
30	547.14 ± 6.94	6.90E81	1.8	0.99885	$\frac{1}{1-1.8} - \frac{(1-\alpha)^{1-1.8}}{1-1.8}$

Standard deviations $S = \sqrt{\sum (X-M)^2/(n-1)}$, where $\sum$ is the sum of, X is the individual score, M is the mean of all scores and n is the sample size (number of scores).

[a] Means ± standard deviations.

for 20 mg ml^{-1},

$$\frac{1}{1-1.7} - \frac{(1-\alpha)^{1-1.7}}{1-1.7}$$

for 30 mg ml^{-1},

$$\frac{1}{1-1.8} - \frac{(1-\alpha)^{1-1.8}}{1-1.8}$$

Compared with an idealized Avrami–Erofeyev equation, a nonintegral value of kinetic exponent n was more appropriate to describe the actual process. The activation energy (E), pre-exponential factor (A), kinetic exponent of the thermal transition and the transition temperature ($T_{d\,max}$) increased with the increase of protein concentration (Tables 1 and 4). This suggested that BSA concentration affected aggregation substantially.

5. Conclusions

The DSC analysis of BSA showed only one characteristic single endothermic transition was detected in all experiments. All the thermal denaturation transitions were found calorimetrically irreversible as reflected by the lack of transition in the second run of all the samples.

The most possible kinetic model was determined by using the master plots method, which indicated that the most possible kinetic models for apparent BSA aggregation at high concentration might be described by using an accommodated Avrami–Erofeyev equation, $G(\alpha) = 1/(1-n) - (1-\alpha)^{1-n}/(1-n)$. Little dependence of the activation energy on the extent of conversion for the apparent BSA aggregation indicated that a simple reaction mechanism with reaction progressing could be used. A simple order reaction model could satisfactorily describe the observed kinetics of BSA aggregation. The observed BSA aggregation at high concentration studied in this paper did not follow rigorously first-order kinetic model or other integral-order reaction models. The denaturation temperature ($T_{d\,max}$), apparent activation energy (E), the apparent order of reaction (n), and pre-exponential factor (A) all increased with the increase of BSA concentration. The differential scanning calorimetric results on transition temperatures and nonisothermal kinetics analysis of the BSA aggregation supported by intrinsic fluorescence indicated the substantial impact of BSA concentration on aggregation.

This study showed the combination of iso-conversional method and the master plots method could be used to model the aggregation mechanism of the protein satisfactorily.

Acknowledgements

This work was financially supported by the National Nature Sciences Foundation of China (Grant Nos. 20373050 and 30600116), Nature Sciences Foundation of Hubei and China Postdoctoral Science Foundation.

References

[1] J.X. Guo, N. Harn, A. Robbins, R. Dougherty, C.R. Middaugh, Biochemistry 4 (2006) 8686.
[2] P.D. Ross, A.P. Minton, J. Mol. Biol. 112 (1977) 437.
[3] W.P. Feil, P.L. Privalov, Biophys. Chem. 4 (1976) 33.
[4] K. Gekko, H. Ito, Biochem. J. 107 (1990) 572.
[5] F. Conejero-Lara, J.M. Sánchez-Ruíz, Eur. J. Biochem. 200 (1991) 663.
[6] S.A. Charman, K.L. Mason, W.N. Charman, Pharm. Res. 10 (1993) 954.
[7] J.C. Martínez, V.V. Filimonov, P.L. Mateo, G. Schreiber, A.L. Fersht, Biochemistry 34 (1995) 5224.
[8] J. Funahashi, K. Takamo, K. Ogosahara, Y. Yamagata, K. Yutani, J. Biochem. 120 (1996) 1216.
[9] M. Weijers, P.A. Barneveld, M.A.C. Stuart, R.W. Visschers, Protein Sci. 12 (2003) 2693.
[10] R. Lumry, H. Eyring, J. Phys. Chem. 58 (1954) 110.
[11] J.E. Kinsella, D.M. Whitehead, Adv. Food Nutr. Res. 33 (1989) 343.
[12] T.J. Peters, All About Albumin Biochemistry, Genetics and Medical Applications, Academic Press, San Diego, CA, 1996.
[13] J.M. Sánchez-Ruíz, J.L. López-Lacomba, M. Cortijo, P.L. Mateo, Biochemistry 27 (1988) 1648.
[14] K. Idakieva, K. Parvanova, S. Todinova, Biochim. Biophys. Acta 1748 (2005) 50.
[15] T. Banerjee, N. Kishore, Thermochim. Acta 411 (2004) 195.
[16] R.F. Epand, R.M. Epand, C.Y. Jung, Biochemistry 38 (1999) 454.
[17] R.L. Remmele Jr., J.Zh. Enk, V. Dharmavaram, D. Balaban, M. Durst, A. Shoshitaishvili, H. Rand, J. Am. Chem. Soc. 127 (2005) 8328.
[18] F. Despa, D.P. Orgill, R.C. Lee, Ann. Biomed. Eng. 33 (2005) 1125.
[19] J.P. Elder, Thermochim. Acta 318 (1998) 229.
[20] S.K. Baier, D.J. McClements, Int. J. Food Sci. Technol. 41 (2006) 189.
[21] S. Baier, D. Julian, McClements, J. Agric. Food Chem. 49 (2001) 2600.
[22] A.K. Burnham, Thermochim. Acta 355 (2000) 165.
[23] S. Vyazovkin, C.A. Wight, J. Phys. Chem. A 101 (1997) 8279.
[24] S. Vyazovkin, C.A. Wight, Thermochim. Acta 340/341 (1999) 53.
[25] S. Vyazovkin, Int. J. Chem. Kinet. 27 (1) (1995) 73.
[26] S. Vyazovkin, Int. J Chem. Kinet. 28 (2) (1996) 95.
[27] S. Vyazovkin, L. Vincent, N. Sbirrazzuoli, Macromol. Biosci. 7 (2007) 1181.
[28] F.J. Gotor, J.M. Criado, J. Malek, N. Koga, F.J. Gotor, J.M. Criado, J. Malek, N. Koga, J. Phys. Chem. A 104 (2000) 10777.
[29] W.J. Tang, Y.W. Liu, X. Yang, C.X. Wang, Ind. Eng. Chem. Res. 43 (2004) 2054.
[30] W.J. Tang, C.X. Wang, D.H. Chen, J. Anal. Appl. Pyrolysis 75 (2006) 49.
[31] W.J. Tang, Y.W. Liu, H. Zhang, C.X. Wang, Thermochim. Acta 408 (2003) 39.
[32] F.J. Gotor, J.M. Criado, J. Malek, N. Koga, J. Phys. Chem. A 104 (2000) 10777.
[33] W.J. Tang, Y.W. Liu, H. Zhang, Z.Y. Wang, C.X. Wang, J. Therm. Anal. Calorim. 74 (2003) 309.
[34] T. Hatakeyama, F.X. Quinn, Thermal Analysis Fundamentals and Applications to Polymer Science, second edition, John Wiley & Sons Ltd., Baffins Lane, Chichester, West Sussex, UK, 1999.
[35] METTLER TOLEDO, Software Option of STAR^e Software, DSC Evaluations 13 Convertion Determination 13-403 Mettler-Toledo GmbH1993-2002 ME-709319G, Printed in Switzerland, 0209/31.12.
[36] A.M. Klibanov, T.J. Ahern, D.L. Oxender, C.F. Fox (Eds.), Thermal Stability of Proteins. In Protein Engineering, Alan R. Liss, New York, 1987, pp. 213–218.
[37] M.A.M. Hoffmann, S.P.F.M. Roefs, M. Verheul, P.J.J.M.v. Mil, K.G.d. Kruif, J. Dairy Res. 63 (1996) 423.
[38] A.C. Alting, R.J. Hamer, C.G. de Kruif, R.W. Visschers, J. Agric. Food Chem. 48 (2000) 5001.
[39] J.W. Park, J. Food Biochem. 14 (1990) 395.
[40] A. Sułkowska, J. Równicka, B. Bojko, W. Sułkowski, J. Mol. Struct. 651–653 (2003) 133.
[41] J.R. Lakowicz, Principles of Fluorescence Spectroscopy, Plenum Press, New York, 1983.

[42] K. Chattopadhyay, S. Mazumdar, Biochemistry 39 (2000) 263.
[43] M. Maciejewski, Thermochim. Acta 355 (2000) 145.
[44] M. Weijers, P.A. Barneveld, M.A. Cohen Stuart, R.W. Visschers, Protein Sci. 12 (2003) 2693.
[45] K. Idakievaa, K. Parvanovaa, S. Todinova, Biochim. Biophys. Acta 1748 (2005) 50.
[46] M.A.M. Hoffmann, J.C. van Miltenburg, J.P. van der Eerden, P.J.J.M. van Mil, C.G. de Kruif, J. Phys. Chem. B 101 (1997) 6988.
[47] A. Stirpe, R. Guzzi, H. Wijma, M.Ph. Verbeet, G.W. Canters, L. Sportelli, Biochim. Biophys. Acta 1752 (2005) 47.
[48] Y. Chen, H. Mao, X. Zhang, Y. Gong, N. Zhao, Int. J. Biol. Macromol. 26 (1999) 129.
[49] A.E. Lyubarev, B.I. Kurganov, V.N. Orlov, H. Zhou, Biophys. Chem. 79 (1999) 199.
[50] A.E. Lyubarev, B.I. Kurganov, J. Therm. Anal. Calorim. 62 (2000) 51.
[51] C. Le Bon, T. Nicolai, D. Durand, Macromolecules 32 (1999) 6120.
[52] J.M. Sanchez-Ruiz, Biophys. J. 61 (1992) 921.
[53] M.L. Galisteo, P.L. Mateo, J.M. Sanchez-Ruiz, Biochemistry 30 (1991) 2061.
[54] R. Jaenicke, Prog. Biophys. Mol. Biol. 49 (1987) 117.